$Cs_3Zr_6Br_{15}Z$ (Z = C, B): A Stuffed Rhombohedral Perovskite Structure of Linked Clusters

Ru-Yi Qi and John D. Corbett*

Department of Chemistry, Iowa State University, Ames, Iowa 50011

Received November 1, 1994[⊗]

The isostructural title compounds are synthesized in good yields from reactions of Zr, $ZrBr_4$, CsBr, and Z in sealed Ta tubing for ~3 weeks at 850 °C. Their single-crystal data refinements established the products as $Cs_{3.02(7)}Zr_6Br_{15}C$ and $Cs_{3.39(5)}Zr_6Br_{15}B$ ($R\bar{3}c$, $Z = 6$, $a = 13.1031(6)$, 13.116(1) Å, $c = 35.800(3)$, 35.980(6) Å, $R(F)/R_w = 5.4/5.9$, 5.4/4.4%, respectively). The structure is derived from a three-dimensional $[Zr_6(Z)Br_{12}]Br_{6/2}$ network of four-rings (as in $ReO_{6/2}$) twisted into a rhombohedral perovskite analogous to VF_3. The three necessary Cs^+ cations are fractionally distributed over five sites that are far from optimal or common, with either eight asymmetric or only three close bromide neighbors. Refinement of a third $Cs_{3.18(5)}Zr_6Br_{15}C$ structure at −50 °C gave the same result with somewhat smaller positional distributions of the atoms.

Introduction

All of the many zirconium cluster halides known within the general type $A^I_x[Zr_6(Z)X^i_{12}]X_n$ ($0 \le x, n \le 6$) appear to require an interstitial heteroatom (Z) in each cluster for stability. Those with three extra halides per cluster ($n = 3$) afford a particularly interesting series structurally because the halide atoms that are always bound at all six zirconium vertices in each cluster must be shared, in this case as $(X^{a\text{-}a})_{6/2}$.[1,2] In fact, the three-dimensional structures found for these exhibit a variety of independent network types in terms of ring size, second-nearest-neighbor cluster interconnections, and angles at $X^{a\text{-}a}$ as well as a range of sites within these arrays for any countercations. The four independent structure types originally described[3−5] were recently expanded first to five by the new tunnel structure of $Rb_5Zr_6Br_{15}Be$[6] and then to six by the unusual $Cs_3(ZrCl_5)Zr_6Cl_{15}Mn$ described in the previous article.[7] The last network type derives from one of the two interpenetrating ReO_3-type lattices that constitute the Nb_6F_{15}[8] structure, as also known for $Li_2Zr_6Cl_{15}Mn$ and $Zr_6Cl_{15}Co$.[5] A "trigonal twist" of the ReO_3 lattice affords a rhombohedral array with room for larger and more numerous cations than possible in Nb_6F_{15}, and this particular $Cs_2Zr_6Cl_{15}Mn$ network also "captures" the novel D_{3h} $ZrCl_5^-$ in what amounts to a stuffed tilted perovskite.[9] The present article reports a novel variation on this with an analogous $Zr_6Br_{15}Z$ network, Z = B, C. In this case, the Cs^+ sites utilized are less than ideal, in part within the cavity formerly occupied by the $ZrCl_5^-$ anion. The dominance of the cluster network in defining the structure is once again in evidence.

Experimental Section

The synthesis and purification of $ZrBr_4$, powdered Zr, and CsBr, the handling of the reactants and products, the reaction techniques in sealed Ta containers, and the characterization procedures, including Guinier X-ray powder pattern techniques, have been described before.[6] The carbon used was from Union Carbide (National Brand), amorphous boron was from Aldrich (five 9's), the zirconium was from Ames Laboratory (reactor grade crystal bar, <500 ppm of Hf), and the Br_2 was an A. D. Mackay product (<0.02% Cl_2). Most reactions were run on a 200−250 mg scale. The identity of the interstitial was established principally through ensuring that its presence was essential to the synthesis of a given phase with specific lattice constants and that a quantitative synthesis, or nearly so, was possible when that component and the composition were correctly identified.

Table 1. Lattice Constants (Å)[a] and Cell Volumes (Å^3) for $Cs_3Zr_6Br_{15}C$ and $Cs_{3.4}Zr_6Br_{15}B$ Phases from Reactions with Different Stoichiometries[b]

stoichiometry	*a*	*c*	*V*
$Cs_2Zr_6Br_{10}C$	13.0862(6)	35.823(4)	5312.8(8)
$CsZr_6Br_9C$[c]	13.1031(6)	35.800(3)	5321.5(7)
$Cs_3Zr_6Br_{15}C$ (30% excess Zr)	13.1010(9)	35.819(5)	5324(1)
$Cs_3Zr_6Br_{15}C$ (15% excess Zr)	13.102(1)	35.784(4)	5320(1)
$Cs_3Zr_6Br_{15}C$	13.088(1)	35.746(5)	5303(1)
$Cs_4Zr_6Br_{15}C$	13.098(1)	35.756(4)	5312(1)
$CsZr_6Br_9B$	13.110(1)	35.96(1)	5351(2)
$Cs_2Zr_6Br_{15}B$	13.104(2)	35.966(4)	5348(1)
$Cs_3Zr_6Br_{15}B$[c]	13.116 (1)	35.980 (6)	5360(2)

[a] $R\bar{3}c$ space group; 22 °C Guinier data with Si as an internal standard. [b] Reactions at 850 °C for 3 weeks. [c] Sources of data crystals.

Synthesis. $Cs_3Zr_6Br_{15}C$ was first observed in the products of reactions with stoichiometries $CsZr_6Br_9C$ and $Cs_2Zr_6Br_{10}C$ that were aimed at more reduced cluster phases and were run for 3 weeks near 850 °C. After a single-crystal study of the carbide, similar reactions loaded for the indicated composition $Cs_3Zr_6Br_{15}Z$ with Z = B, C both gave high yields (>85%, plus Cs_2ZrBr_6 with the carbide) and good single crystals. Although the boride refinement showed a higher cesium content, $Cs_{3.4}Zr_6Br_{15}B$, as expected with the electron-poorer interstitial, subsequent reactions loaded with that stoichiometry yielded none of this phase, rather ~80% of another cluster phase instead that has a higher Cs content, $(Cs_4Br)Zr_6Br_{16}B$.[10] In other words, a slightly lower Cs content appears to be important in obtaining $Cs_{3.4}Zr_6Br_{15}B$. Although the yield of the boride phase increased with added cesium over the series of synthetic results listed in Table 1, the lattice constants did not change much, suggesting that any phase breadth is rather small. On the other hand, the lattice constants of the carbide from reactions run without excess Zr are somewhat smaller than those obtained under more reducing (Zr−rich) conditions. It is conceivable that the evident phase breadth includes a less reduced composition with fewer than three cesium atoms per cluster. This would not be unusual as the clusters therein are particularly electron-rich (see Results).

[⊗] Abstract published in *Advance ACS Abstracts,* March 1, 1995.

(1) Ziebarth, R. P.; Corbett, J. D. *Acc. Chem. Res.* **1989**, *22*, 256.
(2) Corbett, J. D. In *Modern Perspectives in Inorganic Crystal Chemistry*; Parthé, E., Ed.; Kluwer Academic Publishers: Dordrecht, The Netherlands, 1992; p 27.
(3) Ziebarth, R. P.; Corbett, J. D. *J. Am. Chem. Soc.* **1987**, *109*, 4844.
(4) Ziebarth, R. P.; Corbett, J. D. *J. Am. Chem. Soc.* **1988**, *110*, 1132.
(5) Zhang, J.; Corbett, J. D. *Inorg. Chem.* **1991**, *30*, 431.
(6) Qi, R.-Y.; Corbett, J. D., *Inorg. Chem.* **1995**, *34*, 1646.
(7) Zhang, J.; Corbett, J. D. *Inorg. Chem.* **1995**, *34*, 1652.
(8) Schäfer, H.; von Schnering, H.-G.; Niehues, K.-J.; Nieder-Vahrenholz, H. G. *J. Less-Common Met.* **1965**, *9*, 95.
(9) Glazer, A. M. *Acta Crystallogr.* **1972**, *A31*, 756; **1975**, *B28*, 3384.
(10) Qi, R.-Y.; Corbett, J. D. Unpublished research, 1993.

0020-1669/95/1334-1657$09.00/0

Table 2. Selected Crystallographic Data[a]

composition	$Cs_{3.02(7)}Zr_6Br_{15}C$	$Cs_{3.39(5)}Zr_6Br_{15}B$
fw (10^3)	2.159(9)	2.207(7)
space group, Z	$R\bar{3}c$ (No. 167), 6	$R\bar{3}c$ (No. 167), 6
d_{calc}, g cm^{-3}	4.04	4.10
temp, °C	23	22
abs coeff (Mo Kα), cm^{-1}	214.2	212.7
R,[b] %	5.4	5.4
R_w,[b] %	5.9	4.4

[a] Unit cell data are given in Table 1. [b] $R = \sum||F_o| - |F_c||/\sum|F_o|$; $R_w = [\sum w(|F_o| - |F_c|)^2/\sum w(F_o)^2]^{1/2}$, $w = \sigma_F^{-2}$.

Magnetic Susceptibilities. The data were obtained for a ~50 mg ground sample of $Cs_{3.4}Zr_6Br_{15}B$ sealed under He and held between two silica rods in a SiO_2 container. Measurements were made at 3 T over 6−300 K on a Quantum Design MPMS SQUID magnetometer. The data were corrected for the susceptibilities of the container and atom cores.

Single-Crystal Studies. The major features of the Guinier powder pattern of what turned out to be $Cs_3Zr_6Br_{15}C$ appeared similar to those for $Cs_3(ZrCl_5)Zr_6Cl_{15}Mn$,[7] suggesting that some features of the bromide structure might be similar to those of the chloride, yet significant discrepancies in the pattern were also evident. The former turned out to be qualitatively correct. Diffraction data were collected on an Enraf-Nonius CAD4 diffractometer at room temperature from a small, dark purple cylindrical crystal obtained from a $CsZr_6Br_9C$ reaction stoichiometry. The cell initially determined from orientation reflections properly transformed to the correct rhombohedral cell (hexagonal setting). About 1000 reflections first measured without conditions confirmed the R-centering condition without exception. A hemisphere of data collected up to $2\theta = 50°$ with an ω-scan mode supported only the space groups $R3c$ (No. 161) and $R\bar{3}c$ (No. 167). The latter was chosen according to the intensity statistics. Data reduction and absorption correction according to the average of three ψ scans resulted in $R_{ave} = 5.5\%$ for the observed ($3\sigma_I$) data in the corresponding Laue group $\bar{3}m$. The parameters at this stage were consistent with a structural resemblance to $Cs_3(ZrCl_5)Zr_6Cl_{15}Mn$.

The initial model was obtained by direct methods in the SHELXS-86 program package.[11] Since the peak heights of Zr were not significantly different from those of Br, the assignment of correct Zr and Br positions was accomplished mainly by the atom distances around each position. All Zr and Br atoms were correctly located and assigned from the initial output, and a drawing showed a framework very similar to that in $Cs_3(ZrCl_5)Zr_6Cl_{15}Mn$. The differences came out after all the cations were located. A Fourier map calculated after isotropic refinement of all of the Zr and Br atoms gave a prominent peak at the position fully occupied by Cs^+ in the chloride, and with reasonable distances to the adjacent Br atoms, but the position appeared to be only partially occupied (Cs1). The cavity formerly hosting the $ZrCl_5^-$ polyanion in the chloride was virtually empty at this stage. After the anisotropic refinement of all atoms, another peak (~9.4 e/Å^3) was found in the Fourier map in this hole and with ~4 Å distances to the closest non-metal atoms. The assigned Cs2 atoms occur in pairs separated by ~3.3 Å by virtue of a 2-fold axis at $z = 1/4$ (or twinning). The occupancy of the Cs1 position (along with all variables) refined to 76(1)% and that of Cs2 refined to 37(2)%, yielding the $Cs_{3.02(7)}Zr_6Br_{15}C$ empirical formula.

The refinement converged at $R = 5.4\%$, $R_w = 5.9\%$. The final difference Fourier map contained only small residuals, 3.9 e/Å^3 located 0.35 Å (~$\vec{c}$) from the oversized Cs2 and 3.51 e/Å^3 that was 2.2−2.4 Å from both Cs1 and Cs2. These were about 2 e/Å^3 above background. As will be described later, Cs2 occurs in a very open and asymmetric environment that is doubtlessly responsible for the ellipsoidal characteristics and, in part, these residuals.

Both Cs atoms were more localized when the carbide structure was refined with a data set collected at −50 °C from a somewhat larger crystal produced in a reaction loaded as $Cs_2Zr_6Br_{10}C$. The refined composition was $Cs_{3.18(5)}Zr_6Br_{15}C$, with the cation contents shifting in favor of the Cs1 site. The errors in the positional and thermal parameters of the atoms were all smaller, and the principal axes for the Zr and Br ellipsoids decreased 15−50%, while those of Cs1 and Cs2 were smaller by 10−45% and 70−90%, respectively. The larger crystal gave 40% more observed (weak) reflections, and higher residuals (7.1, 7.5%), in part because of apparent streaks of scattering along c^*, made $F_o > F_c$ for many hkl reflections that lay in the "shadow" of intense reflections (results in supplementary material).

(11) Sheldrick, G. M. SHELXS-86. Universität Göttingen, Germany, 1986.

Table 3. Positional and Isotropic Displacement Parameters for $Cs_{3.02(7)}Zr_6Br_{15}C$ and $Cs_{3.39(5)}Zr_6Br_{15}B$[a]

atom	psn	x	y	z	B_{eq},[b] Å^2
			$Cs_{3.02(7)}Zr_6Br_{15}C$		
Zr	36*f*	0.0094(2)	0.1467(2)	0.03700(6)	1.2(1)
Br1	36*f*	0.1711(3)	0.1609(3)	0.08538(8)	2.0(1)
Br2	36*f*	0.3308(3)	0.1521(3)	0.0007(1)	2.0(1)
Br3	18*e*	0.6506(3)	0	1/4	1.9(2)
C	6*b*	0	0	0	2(1)
Cs1[c]	18*d*	1/2	0	0	12.3(5)
Cs2[d]	12*c*	0	0	0.2964(7)	17(2)
			$Cs_{3.39(5)}Zr_6Br_{15}B$		
Zr	36*f*	0.0075(2)	0.1481(2)	0.03754(6)	0.86(8)
Br1	36*f*	0.1702(3)	0.1618(3)	0.08504(8)	1.6(1)
Br2	36*f*	0.3304(3)	0.1552(3)	0.0007(1)	1.5(1)
Br3	18*e*	0.6531(4)	0	1/4	1.6(3)
B	6*b*	0	0	0	2(2)
Cs1[e]	18*d*	1/2	0	0	7.8(3)
Cs2[f]	12*c*	0	0	0.3021(5)	6.6(7)

[a] Space group $R\bar{3}c$, hexagonal setting. [b] $B_{eq} = (8\pi^2/3)\sum_i\sum_j U_{ij}a_i^*a_j^*\vec{a}_i\vec{a}_j$. [c] 76(1)% occupied. [d] 37(2)% occupied. [e] 93.1(9)% occupied. [f] 30(1)% occupied.

The refinement of the very similar structure for the boride-centered analogue at room temperature yielded $R = 5.4\%$, $R_w = 4.4\%$ and a composition $Cs_{3.39(5)}Zr_6Br_{15}B$, additional cesium appearing in the Cs1 position. The Cs ellipsoids were still disparate, but 40−80% of those refined for the carbide. The largest residual electron densities were small peaks of 3.0 and 2.9 e/Å^{-3} that were 2.5 and 2.2 Å from Cs2, respectively. As in all structures studied, the Fourier maps of both cation regions showed only single, broad maxima (supplementary material).

The positional parameters and isotropic-equivalent ellipsoid data for the carbide and boride structures at room temperature are listed in Table 3. More crystallography details, the results of the low-temperature study of the carbide, and the anisotropic parameters for the three structures are contained in the supplementary material; these and the structure factor data are also available from J.D.C.

Results and Discussion

The particular structural connectivities achieved between M_6X_{12} building blocks are largely determined by the amount of excess halide (beyond 12), and this factor appears to be the major and structure-determining feature. In common with all $(M_6X^i_{12})X^{a\text{-}a}{}_{6/2}$ cluster structures, the three additional bromine atoms in $Cs_3[(Zr_6(Z)Br_{12})]Br^{a\text{-}a}{}_{6/2}$ (Z = B, C) bridge between vertices in adjoining clusters to link these into a three-dimensional network. The specific arrangement obtained depends as well on both the cluster sizes (as defined by the metal, halogen, and interstitial) and, especially, the number and sizes of the cations that must also be accommodated. The number of cations is in turn driven by electronic requirements of the cluster itself, particularly the number of valence orbitals in and electron count of the interstitial.[1,2] Inclusion of cesium in the present syntheses of $Zr_6(Z)Br_{15}$-type phases together with the inherent stability of the 16-e cluster under strongly reducing conditions mean a relatively open three-dimensional anionic array is necessary for the three cations.

Figure 1 shows the [110] projection of the $Cs_3Zr_6Br_{15}C$ result. (This portion is useful since it contains all components of the structure, including the R-centering characteristics; in this case the Cs1 atoms lie outside the actual [110] section.) Clusters centered by carbon at (0, 0, 0) and Cs2 near a 2-fold axis at z

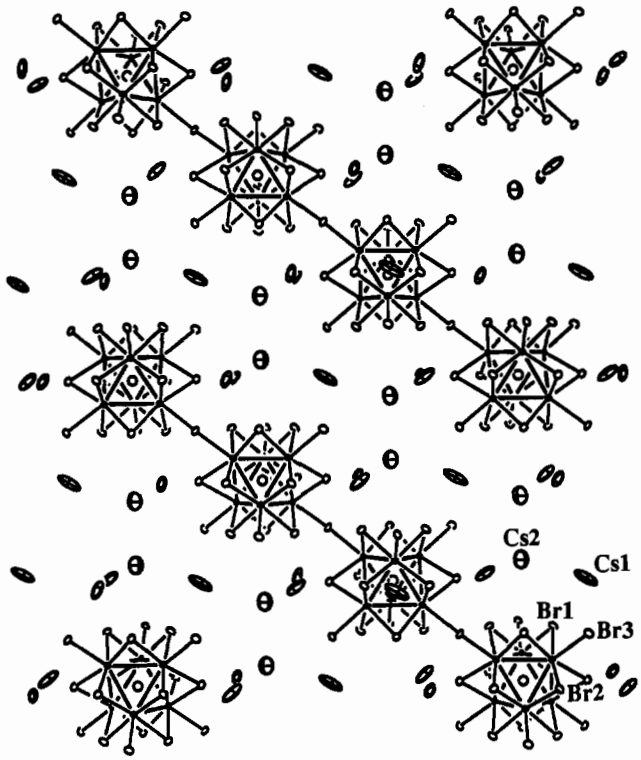

Figure 1. [110] section of the structure of $Cs_3[Zr_6(Z)Br_{12}]Br_{6/2}$, Z = C, B, with all Zr−Br bonds marked ($\vec{c}$ vertical, 50% probability ellipsoids). The pair of Cs2 atoms surround the body center of a rhombohedral perovskite structure (0, 0, $^1/_4$).

$= {}^1/_4$ both lie on the vertical 3-fold axes while Cs1 in this section lies on an inversion center at ($^1/_6$, $^5/_6$, $^1/_3$) and equivalent. The clear three-layer ccp (*R*-centered) arrangement of clusters is doubled by the *c*-glide in (110) (and elsewhere), which means that the clusters in the upper half of the cell occur with the opposite orientation. (This is necessary to give coherence to the intercluster bridging mode (below).) Twelve layers stacked normal to $\vec{c}$ are fairly well defined by (a) the bridging Br1 plus the Br2 atoms at the upper and lower boundaries of each cluster (layers near $z = {}^1/_{12}$, $^1/_4$, $^5/_{12}$, ...) and (b) layers at 0, $^1/_6$, $^1/_3$ ... composed of Br3 atoms about the waist of each cluster plus the carbon interstitial, all Cs1 atoms, and, somewhat displaced, the Cs2 atoms. The last two lie around a large cavity centered in this layer, as will be described later. The overall cation disposition contrasts with that in other cluster halide structures with rhombohedral packing in which the cations are frequently bound in antiprismatic cavities between roughly close-packed halide layers, e.g., in $Cs_2Zr_6I_6{\cdot}Zr_6I_{12}C$[12] and $Ba_3Zr_6Cl_{18}Be$.[13]

Description of the $(Zr_6(C)Br_{12})Br_{6/2}$ backbone of the structure is useful before the cation binding is described and compared. The network can be readily related to a primitive cubic ReO_3 lattice or, instead, one of the two interpenetrating but not interconnected networks in Nb_6F_{15} that become geometrically possible when rhenium is replaced by the larger Nb_6F_{12} clusters. This pair of lattices accommodate nothing larger than lithium cations in the $Li_2Zr_6Cl_{15}Mn$ analogue,[5] but fortunately, a twisted version of the single ReO_3 network is retained when larger cesium (but not rubidium) cations are included in certain chloride or bromide examples. Figure 2 shows both a [111] view of the primitive $(Nb_6F_{12})F_{6/2}$ (or $[Zr_6(Co)Cl_{12}]Cl_{6/2}$[5]) portion (left) and its relationship to the [001] section of $Zr_6(Z)Br_{12}Br_{6/2}$ (Z = C, B) (right). (The 12 inner halides on each cluster are omitted throughout for clarity.) Rotation of the central and the outer six clusters on the left in opposite directions by ~23° introduces a bend in the formerly linear $Br^{a\text{-}a}$ bridge of twice as much and an angle of 134° (Table 4). (The Z−Zr−$Br^{a\text{-}a}$ angle also deviates from 180 ° by ~1.2°.)

Table 4. Important Bond Distances (Å) and Angles (deg) for $Cs_{3.02(7)}Zr_6Br_{15}C$ and $Cs_{3.39(5)}Zr_6Br_{15}B$

		$Cs_{3.02(7)}Zr_6Br_{15}C$	$Cs_{3.39(5)}Zr_6Br_{15}B$
		Distances	
Zr−Zr	×2	3.228(4)	3.283(4)
	×2	3.239(4)	3.300(4)
$\bar{d}$		3.234	3.292
Zr−Z	×1	2.286(2)	2.327(2)
Zr−Br1^i	×1	2.671(4)	2.669(4)
	×1	2.681(4)	2.672(4)
Zr−Br2^i	×1	2.687(4)	2.681(4)
	×1	2.688(4)	2.682(4)
Zr−Br3$^{a\text{-}a}$	×1	2.920(3)	2.904(3)
Cs1^a−Br1	×2	3.582(3)	3.616(3)
−Br2	×2	3.648(3)	3.690(3)
	×2	3.948(3)	3.918(3)
−Br3	×2	3.765(2)	3.767(2)
$\bar{d}$		3.736	3.748
Cs2^a−Br1	×3	4.029(9)	3.977(6)
Cs2−Cs2^a	×1	3.32(4)	3.75(3)
		Angles	
Zr−Zr−Zr	×2	60.00	60.00
	×2	60.11(5)	60.17(4)
Zr−Br3−Zr	×1	134.3(2)	134.0(2)
Br1−Zr−Br2	×2	164.0(1)	165.8(1)
	×2	164.2(1)	165.9(1)
Br3−Zr−Z	×1	178.6(1)	178.8(1)

[a] Cs1 and Cs2 sites are fractionally occupied; see Table 3.

The resulting lattice also exhibits a nearly hcp array of the $Br^{a\text{-}a}$ atoms, and it falls conveniently in the family of compounds and structure types all derived by such twists of the aristotypic cubic perovskite structure.[14] The present rotations are close in magnitude to those in VF_3 where, of course, there are neither countercations to be accommodated nor room for them. The $R\bar{3}c$ space group also defines the structure as characteristic of several tilted rhombohedral perovskites.[9] In the present case, a small elongation of the parent cubic lattice along [111] occurs in the process, presumably because of cation size requirements. Thus, the equivalent rhombohedral α angle (the cis intercluster angle along $\vec{c}$) is 85.7° (carbide) or 85.5° (boride) at room temperature, which means the cell is elongated by ~7.4% along c_H beyond the ideal cubic equivalent. The clusters as well as Zr−$Br^{a\text{-}a}$ bridging distances remain almost unchanged during this conformation change. The small elongation of the metal clusters along the $\bar{3}$ axis is not significant (by 0.011(6) and 0.017(6) Å in Zr−Zr), while the Zr−Z distances are typical.[4,10]

In contrast to the ReO_3 or VF_3 examples, this cluster network presents a surface of Br^i atoms about the $Zr_6(Z)$ clusters and anionic $Br^{a\text{-}a}$ bridges to the cavities within. Our synthetic conditions have forced the structure to accommodate three (or more) large unipositive countercations through the choice of the interstitial coupled with the fortuitous stabilities of both the 16-e carbide and 15.4-e boride clusters and this particular $[(Zr_6(Z)X_{12})]X_{6/2}$ network. It is at this point that the similarities to and differences from the structure of $Cs_3(ZrCl_5)Zr_6(Mn)Cl_{12}Cl_{6/2}$ described in the preceding article[7] merit attention. The anionic networks are substantially identical. Although the Mn interstitial is somewhat larger than C or B, the larger bromide is more

(12) Payne, M. W.; Corbett, J. D. *J. Solid State Chem.* **1993**, *102*, 553.
(13) Zhang, J.; Corbett, J. D. *Z. Anorg. Allg. Chem.* **1991**, *598/599*, 363.
(14) Chapuis, G. C. in *Modern Perspectives in Inorganic Crystal Chemistry*; Parthé, E., Ed.; NATO ASI Series C; Kluwer Academic Publishers: Dordrecht, The Netherlands, **1992**; p 1.

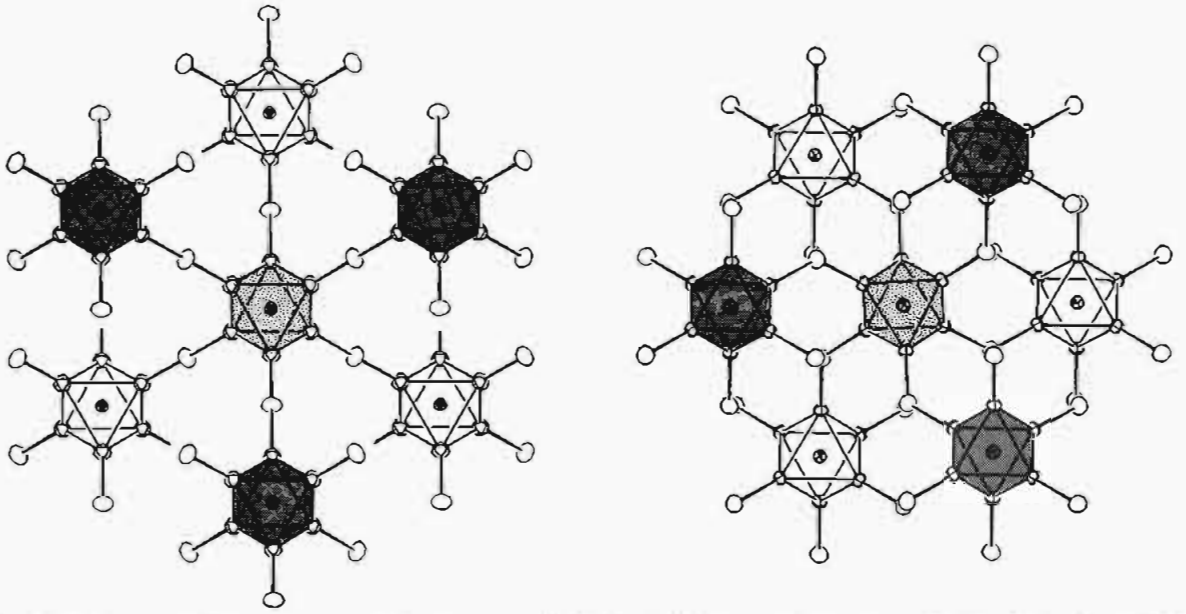

Figure 2. The "trigonal twist" that carries the primitive lattice in $(Nb_6F_{12})F_{6/2}$ ([111] view) (left) into that of the $(Zr_6(Z)Br_{12})Br_{6/2}$ ([001]) (right). The shading distinguishes ccp clusters at different levels in each. All inner halides have been omitted.

important as far as lattice dimensions. In addition, the expansions of the networks along $\bar{c}$ relative to the ideal cubic array (6.7% chloride, 7.4% bromide) and the twist at X^{a-a} (133.4, 134.3°) are also similar, and both accommodate cesium cations in an 18*d* site with inversion symmetry ($^1/_2$, 0, 0, etc.). However, the remainder of the features are strikingly different. The remarkable $Cs_3(ZrCl_5)Zr_6Cl_{15}Mn$ contains the new and relatively large trigonal bipyramidal $ZrCl_5^-$ anion centered on the 32 site at 0, 0, $^1/_4$, etc. (Figure 1). This is the B site in ABX_3 perovskites, making this an unusual example of a rhombohedral (equitilted) perovskite that contains a centered *anion* and is further stuffed with cesium. The five chlorines in the simple $ZrCl_5^-$ complex are not members of the cluster network but still provide one-third of the chlorine neighbors about each Cs1, the remainder coming from six Cl^i and two Cl^{a-a}. The good "fit" of $ZrCl_5^-$ on the 3-fold axes in this structure must be important to its "capture".

In the $Cs_{\sim 3}Zr_6Br_{15}Z$ examples, the cluster framework remains dominant, and the necessary cations must be accommodated in more marginal ways relative to common and optimal environments for Cs^+. This has been found to be a common aspect of many quaternary cluster compounds, the driving forces for a particular structure appearing to come from the element centering the cluster and the X:Zr ratio utilized as this determines the network characteristics via the number of exo halogens. The cation sites utilized, particularly for the larger ions, frequently appear to be what is left over, even when the environments are oversized, asymmetric, or defined by only a few halogens.[1-3,10,15-17] The ZrX_5^- removal from within the cluster network leaves a cavity ~5 × 9 Å within the bromide lining, and the same three Cs^+ cations per cluster are now fractionally distributed among five sites, the same 18*d* ($\bar{1}$) position plus a 12*c* (3) site within the cavity left by that polyanion, with a distinct preference for the former. The loss of Cl4 and Cl5 members of $ZrCl_5^-$ also leaves a quite asymmetric coordination of Cs1 by only eight bromines at distances of 3.58−3.95 Å, Figure 3, and the site is occupied about ~76% of the time. The large and elongated ellipsoid for Cs1 that was refined in all

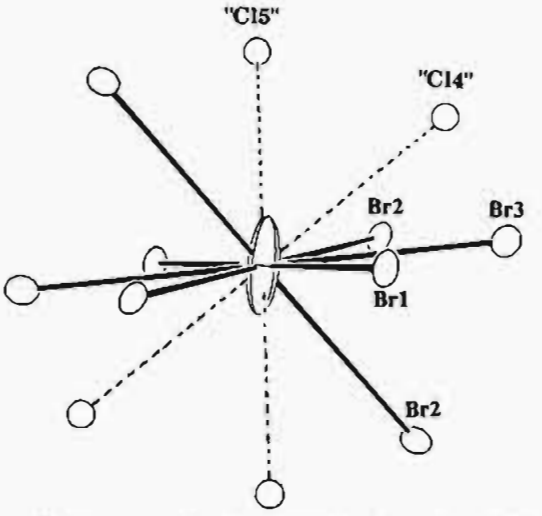

Figure 3. Environment of the 18*d* ($\bar{1}$) Cs1 site in $Cs_{3.4}Zr_6Br_{15}B$. Dashed lines connect the additional chlorine atoms that are present in the $ZrCl_5$ unit in $Cs_3(ZrCl_5)Zr_6Cl_{15}Mn$. (50%).

three structures, with extreme ratios of 5.5−6.8:1 in principal axes, is not particularly surprising in light of Figure 3. The average Cs−Br distances, 3.736 and 3.748 Å in the carbide and boride, respectively, compare fairly well with the crystal radius sum for an eight-coordinate Cs, 3.70 Å.[18] A Fourier map section through Cs1 in the boride shows a single resolvable maximum, while a −50 °C data set for $Cs_{3.18(5)}Zr_6Br_{15}C$ gave U_{ii} values for Cs1 about half as large but very similarly proportioned (supplementary material).

The competing Cs2 position is, by contrast, very poorly bounded and occupied about 37% of the time in the carbide, ~30% in the cesium-richer boride ($Cs_{3.39(5)}Zr_6Br_{15}B$) (Figure 4) where the additional cations are found in the Cs1 site (93-(1)%). These changes reflect the competition of two fairly poor sites for cesium binding, and Cs2 does not attain more than about one-third occupancy. The reasons for this are evident in Figure 4 (and Figure 1) where Cs2 is seen to lie nearly in the plane of just three waist Br2 atoms ($z = ^1/_6$, etc.) on surrounding

(15) Ziebarth, R. P.; Corbett, J. D. *J. Am. Chem. Soc.* **1989**, *111*, 3272.
(16) Imoto, H.; Simon, A. Unpublished research, 1980.
(17) Ziebarth, R. P.; Corbett, J. D. *Inorg. Chem.* **1989**, *28*, 626.
(18) Shannon, R. P. *Acta Crystallogr.* **1976**, *A32*, 751.

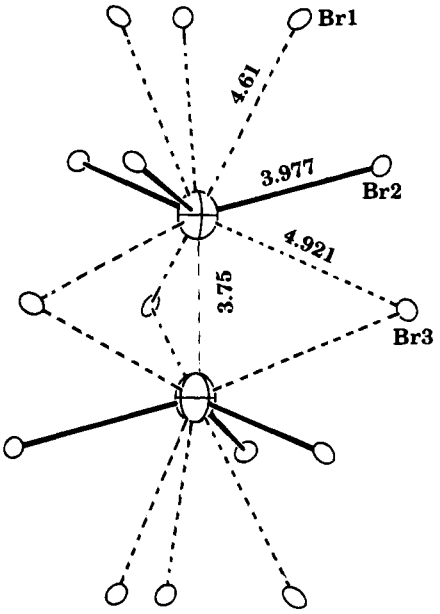

Figure 4. A pair of Cs2 sites, each ~30% occupied, in $Cs_{3.4}Zr_6Br_{15}B$ (C_3 axis vertical). Br1 and Br3 atoms lie about the waists of and between $Zr_6(B)Br_{12}$ clusters, respectively (50%).

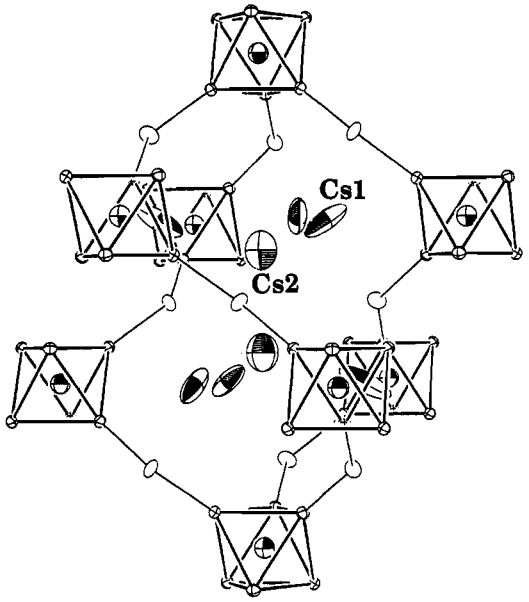

Figure 5. The perovskite "B" site around (0, 0, 1/4) that contains Cs1 and Cs2 in $Cs_{3.4}Zr_6Br_{15}B$ (80%) (Br^i atoms on each cluster omitted).

clusters, but these are nearly 4.00 Å away (vs 3.75 Å for eight Br about Cs1). Their second nearest neighbors are all 4.6 Å or more removed. The Cs2 atoms refine as pairs because of 2-fold axes at x, 0, 1/4, etc. that appear applicable to the rest of the structure; the actual Cs2 distributions are doubtlessly correlated. The refined ellipsoids are accordingly large but less asymmetric than that for Cs1. Note that the bromine atoms show no significant problems in their ellipsoids. The dispositions of the two cation sites within the cavity around 0, 0, 1/4 are demonstrated in Figure 5. The Cs2 occupancies are probably not particularly well determined, and their positions would appear to reflect longer range Coulombic effects as well. Direct analyses are precluded by the lack of either a quantitative yield (see Experimental Section) or a means of fractionation of the product.

The clusters in the carbide product $Cs_{3.0}Zr_6Br_{15}C$ have 16 cluster-based electrons, $(3 \times 1 + 6 \times 4 + 4 - 15 \times 1)$, whereas those in the boride $Cs_{3.4}Zr_6Br_{15}B$ contain about 15.4 electrons.

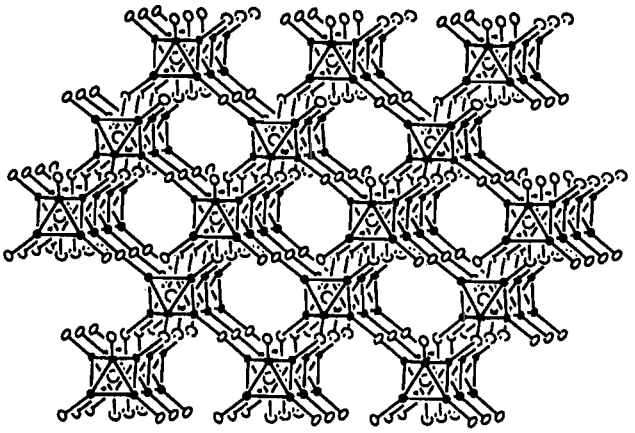

Figure 6. One set of the tunnels in $Cs_3Zr_6Br_{15}C$ (Cs omitted; ~[010] view, 90% ellipsoids).

The cesium limit in the latter illustrates something of the problem of accommodating more cations in this lattice as well as the intrinsic stability of this cluster (below). (Although the particular synthetic system that produced the boride crystal was also less reduced than for the carbide, Table 1 shows that the boride exhibits virtually no stoichiometry range even when excess zirconium is present. Note also that ZrC or ZrB_2 does not provide suitable competition with cluster formation.) Systems that are cesium-richer than $Cs_3Zr_6Br_{15}B$ do not give a more reduced boride, rather only another phase that is novel in its own right, $(Cs_4Br)Zr_6Br_{16}B$, with a novel isolated bromide.[10] It should be noted that rubidium can evidently not be bound in the present structure, perhaps because the cation sites are too large, these compositions giving another network (tunnel) structure $Rb_{\sim 4}Zr_6Br_{15}B$ and an unknown carbide.[6]

As in many structures, the presence of (small) tunnels lined by cesium can also be discerned in the present example (without special glasses). One example is shown in Figure 6 nearly along [010], and another with cesium cations, in the synopsis in the Table of Contents. Such tunnels defined by a spiral array of linked clusters can be perceived every 60° in the basal plane in Figures 1 (right) and 5.

An approximate verification of the composition and degree of reduction of the boride cluster was also obtained from magnetic studies. A nonlinear least-squares fit to the susceptibility of a sample of about 85% purity yielded a χ_{TIP} (van Vleck) term of 5.4×10^{-4} cgsu mol^{-1}, very comparable to values for many $(M_6Cl_{12})Cl_n$ cluster compounds of niobium and tantalum[19] as well as other bromides.[10] The temperature-dependent portion yielded a μ_{eff} value of 0.58(4) μ_B, in reasonable agreement with expectation for ~0.61 unpaired electron when the compositional uncertainty is also considered. Quenching of the moment was evident below 130 K, possibly because of spin−orbit coupling.

The 16-e cluster found in $Cs_3Zr_6Br_{15}C$ may at first thought seem unusual since 14 e in zirconium clusters centered by main-group elements is both the expectation[20] and the general observation. Thus, there are only a couple of 15-e examples in all $Zr_6Cl_{12}Z$-type cluster phases.[4] On the other hand, $Zr_6I_{12}C$ contains 16-e clusters and 15-e members include $AZr_6I_{14}C$, $Zr_6I_{12}B$, and $Zr_6I_{14}P$.[21,22] The 15-e $CsZr_6Br_{14}C$ and $Zr_6Br_{12}B$ are also known among the less extensively investigated bro-

(19) Converse, J. G.; McCarley, R. E. *Inorg. Chem.* **1970**, *9*, 1361.
(20) Hughbanks, T. *Prog. Solid State Chem.* **1989**, *19*, 329.
(21) Smith, J. D.; Corbett, J. D. *J. Am. Chem. Soc.* **1985**, *107*, 5704; **1986**, *108*, 1927.
(22) Rosenthal, G.; Corbett, J. D. *Inorg. Chem.* **1988**, *27*, 53.

mides.[23] In contrast, 15- and 16-e members of (uncentered) niobium chloride cluster compounds are relatively common. These contrasts vis-à-vis the normal 14-e state have been generally interpreted in terms of matrix effects, namely, the result of the withdrawal of the metal vertices from the planes of the four adjoining X^i atoms that is favored with small M, small Z, or large X.[4] These changes serve to diminish the π^* components of the otherwise bonding LUMO a_{2u}, making it more accessible for occupancy by one or two more electrons. The trans X^i-Zr-X^i angles at each vertex are one measure of this distortion, and the 164° values in $Cs_3Zr_6Br_{15}C$ put it in the upper range known for zirconium iodides and among the niobium chlorides, but below the spread among zirconium chloride carbides (167−171°). Of course, the particular lattice, especially the binding of any countercations, must provide important secondary factors regarding stability. The larger boride interstitial should naturally mean a lessened tendency for further reduction, as observed and in parallel with the seeming difficulty of bonding more cations in this unusual structure.

Acknowledgment. This work was supported by the National Science Foundation, Solid State Chemistry, via Grant DMR-9207361 and was carried out in the facilities of Ames Laboratory, U.S. Department of Energy.

Supplementary Material Available: Tables of data collection and refinement details, positional parameters and distances for the cluster carbide at −50 °C, and anisotropic displacement parameters for the three structures and figures showing electron density sections for the cation regions in the boride (6 pages). Ordering information is given on any current masthead page.

IC9412567

(23) Ziebarth, R. P.; Corbett, J. D. *J. Solid State Chem.* **1989**, *80*, 56.